Advanced International Journal for Research (AIJFR)
E-ISSN: 3048-7641 ● Website: www.aijfr.com ● Email: editor@aijfr.com

Design and implementation speed control system of DC Motor using Thyristor in MATLAB Simulink

Abhishek Kumbhar[1], Tanmay Patle[2]

[1,2] Student, School of Electrical and Electronics Engineering, Dr Vishwanath Karad MIT World Peace University, Pune, Maharashtra, India

Abstract

This paper presents a simple and effective method for controlling the speed of a DC motor using a single-phase controlled rectifier (SCR bridge). The output voltage supplied to the motor is regulated by adjusting the firing angle of the SCRs, which directly changes the armature voltage and controls the motor speed. A triggering circuit generates accurate gate pulses, while a feedback mechanism measures the actual motor speed and corrects any error through a PI-based controller. This closed-loop approach ensures stable operation, smooth speed variation, and improved performance under different load conditions. The proposed system is low-cost, easy to implement, and suitable for industrial as well as educational applications.

Keywords: DC Motor, Speed Control, Thyristor, Firing Angle, MATLAB Simulink

1. Introduction

Although a far greater percentage of electric motors in service are AC. motors, the DC motor is of considerable industrial importance. The principal advantage of a DC motor is that its speed can be changed over a wide range by a variety of simple methods (Abdessamad Intidam, 2023). Such a fine speed control is generally not possible with AC motors. In fact, fine speed control is one of the reasons for the strong competitive position of DC. motors in the modem industrial applications. In this chapter, we shall discuss the various methods of-speed control of DC motors.

- Speed Control of DC Motors

The speed of a DC motor is given by:

$$N \alpha \frac{E_b}{\emptyset}$$

$$or \quad N = K\frac{(V - I_a R)}{\emptyset} \; r.p.m \qquad \text{(i)}$$

$$where \quad R = R_a \qquad for\ Shunt\ Motor$$

$$R = R_a + R_{se} \qquad for\ Series\ Motor$$

From exp. (i), it is clear that there are three main methods of controlling the speed of a DC motor, namely:

(i) By varying the flux per pole. This is known as flux control method.
(ii) By varying the resistance in the armature circuit. This is known as armature control method.
(iii) By varying the applied voltage V. This is known as voltage control method.

Speed Control of D.C. Shunt Motors

The speed of a shunt motor can be changed by

(i) Flux control method
(ii) Armature control method
(iii) Voltage control method. The first method (i.e. flux control method) is frequently used because it is simple and inexpensive (Al-Falahi1, 2008).

1. Flux control method

It is because by varying the flux, the motor speed can be changed and hence the name flux control method. (Arpita Banik, 2023) In this method, a variable resistance (known as shunt field rheostat) is placed in series with shunt field winding as shown in Fig. 1.1.

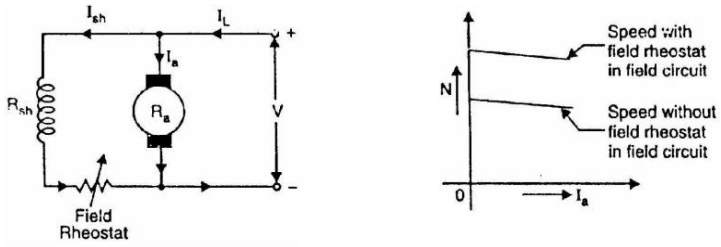

Fig. 1

The shunt field rheostat reduces the shunt field current and hence the flux. Therefore, we can only raise the speed of the motor above the normal speed See Fig. 1.2. Generally, this method permits to increase the speed in the ratio 3:1. Wider speed ranges tend to produce instability and poor commutation.

Advantages

1. This is an easy and convenient method.
2. It is an inexpensive method since very little power is wasted in the shunt field rheostat due to relatively small value.
3. The speed control exercised by this method is independent of load on the machine.

Disadvantages

1. Only speeds higher than the normal speed can be obtained since the total field circuit resistance cannot be reduced below the shunt field winding resistance.
2. There is a limit to the maximum speed obtainable by this method. It is because if the flux is too much weakened, commutation becomes poorer.

Note. The field of a shunt motor in operation should never be opened because its speed will increase to an extremely high value.

2. Armature control method

This method is based on the fact that by varying the voltage available across the armature, the back e.m.f and hence the speed of the motor can be changed (George, 2008). This is done by inserting a variable resistance RC (known as controller resistance) in series with the armature as shown in Fig. (2.1).

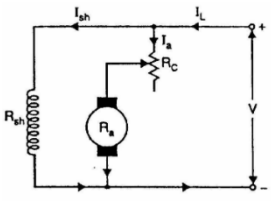

Fig. 2.1

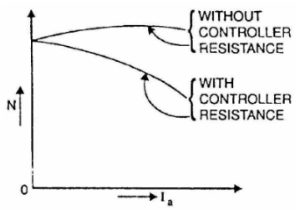

Fig. 2.2

$$N \propto V - I_a(R_a + R_c) \qquad \text{(ii)}$$

$$where, \quad R_c = controller\ resistance$$

Due to voltage drop in the controller resistance, the back e.m.f. is decreased. Since $N \propto E_b$, the speed of the motor is reduced. The highest speed obtainable is that corresponding i.e., normal speed. Hence, this method can only provide speeds below the normal speed See Fig. 2.2.

Disadvantages

1. A large amount of power is wasted in the controller resistance since it carries full armature current I_a .
2. The speed varies widely with load since the speed depends upon the voltage drop in the controller resistance and hence on the armature current demanded by the load.
3. The output and efficiency of the motor are reduced.
4. This method results in poor speed regulation

Due to above disadvantages, this method is seldom used to control tie speed of shunt motors.
Note. The armature control method is a very common method for the speed control of DC series motors. The disadvantage of poor speed regulation is not important in a series motor which is used only where varying speed service is required.

3. Voltage control method

In this method, the voltage source supplying the field current is different from that which supplies the armature. This method avoids the disadvantages of poor speed regulation and low efficiency as in armature

control method. However, itis quite expensive. Therefore, this method of speed control is employed for large size motors where efficiency is of great importance (Hashmia S. Dakheel1, 2022).

Multiple voltage control. In this method, the shunt field of the motor is connected permanently across a-fixed voltage source. The armature can be connected across several different voltages through a suitable switchgear. In this way, voltage applied across the armature can be changed. The speed will be approximately proportional to the voltage applied across the armature. Intermediate speeds can be obtained by means of a shunt field regulator.

Ward-Leonard system. In this method, the adjustable voltage for the armature is obtained from an adjustable-voltage generator while the field circuit is supplied from a separate source. This is illustrated in Fig. (3.1). The armature of the shunt motor M (whose speed is to be controlled) is connected directly to a D.C generator G driven by a constant-speed A.C motor A. The field of the shunt motor is supplied from a constant-voltage exciter E. The field of the generator G is also supplied from the exciter E. The voltage of the generator G can be varied by means of its field regulator. By reversing the field current of generator G by controller FC, the voltage applied to the motor may be reversed. Sometimes, a field regulator is included in the field circuit of shunt motor M for additional speed adjustment. With this method, the motor may be operated at any speed up to its maximum speed (Ling Xu, 2016).

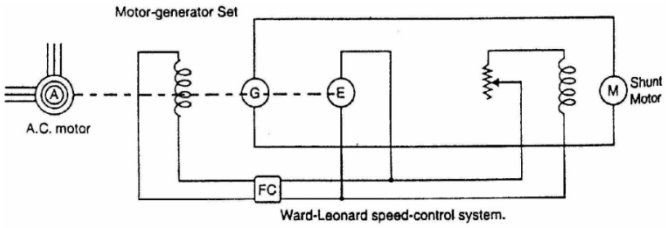

Fig. 3.1

Advantages

1. The speed of the motor can be adjusted through a wide range without resistance losses which results in high efficiency.
2. The motor can be brought to a standstill quickly, simply by rapidly reducing the voltage of generator G. When the generator voltage is reduced below the back e.m.f. of the motor, this back e.m.f. sends current through the generator armature, establishing dynamic braking. While this takes place, the generator G operates as a motor driving motor A which returns power to the line.
3. This method is used for the speed control of large motors when a d.c. supply is not available.

The disadvantage of the method is that a special motor-generator set is required for each motor and the losses in this set are high if the motor is operating under light loads for long periods.

4. Types of D.C. Motor Starters

The stalling operation of a DC motor consists in the insertion of external resistance into the armature circuit to limit the starting current taken by the motor and the removal of this resistance in steps as the motor accelerates. When the motor attains the normal speed, this resistance is totally cut out of the

armature circuit. It is very important and desirable to provide the starter with protective devices to enable the starter arm to return to OFF position.

1. When the supply fails, thus preventing the armature being directly across the mains when this voltage is restored. For this purpose, we use no-volt release coil.
2. When the motor becomes overloaded or develops a fault causing the motor to take an excessive current. For this purpose, we use overload release coil.

There are two principal types of D.C motor starters viz., three-point starter and four-point starter. As we shall see, the two types of starters differ only in the manner in which the no-volt release coil is connected (M. SRI-JAYANTHA, 1984).

5. IGBT Basics

Recent technology advances in power electronics have arisen primarily from improvements in semiconductor power devices, with insulated gate bipolar transistors (IGBT) leading the market today for medium power applications. IGBTs feature many desirable properties including a MOS input gate, high switching speed, low conduction voltage drops, high current carrying capability, and a high degree of robustness. Devices have drawn closer to the 'ideal switch', with typical voltage ratings of 600 - 1700 volts, on-state voltage of 1.7 - 2.0 volts at currents of up to 1000 amperes, and switching speeds of 200 - 500 ns.

The availability of IGBTs has lowered the cost of systems and enhanced the number of economically viable applications. The insulated gate bipolar transistor (IGBT) combines the positive attributes of BJTs and MOSFETs. BJTs have lower conduction losses in the on-state, especially in devices with larger blocking voltages, but have longer switching times, especially at turn-off while MOSFETs can be turned on and off much faster, but their on-state conduction losses are larger, especially in devices rated for higher blocking voltages. Hence, IGBTs have lower on-state voltage drop with high blocking voltage capabilities in addition to fast switching speeds.

IGBTs have a vertical structure as shown in Fig. 5.1. This structure is quite similar to that of the vertical diffused MOSFET except for the presence of the p+ layer that forms the drain of the IGBT. (Mrs Khin Ei Ei Khine, 2019)This layer forms a p-n junction (labeled J1 in the figure), which injects minority carriers into what would appear to be the drain drift region of the vertical MOSFET. The gate and source of the IGBT are laid out in an inter-digitated geometry similar to that used for the vertical MOSFET.

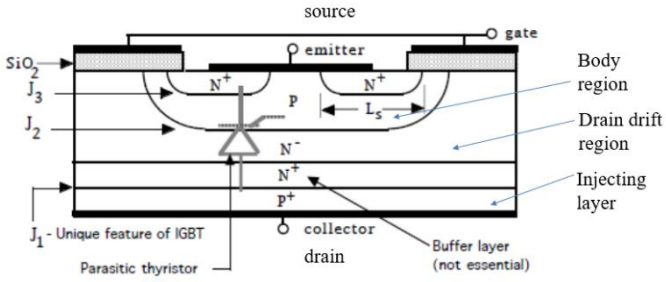

Fig. 5.1 Physical structure of an IGBT

The IGBT structure shown in Fig. 5.1 has a parasitic thyristor which could latch up in IGBTs if it is turned on. The n + buffer layer between the p + drain contact and the n + drift layer, with proper doping density and thickness, can significantly improve the operation of the IGBT, in two important respects.

It lowers the on-state voltage drop of the device and, and shortens the turnoff time. On the other hand, the presence of this layer greatly reduces the reverse blocking capability of the IGBT. The circuit symbol for an n-channel IGBT is shown in Fig. 5.2

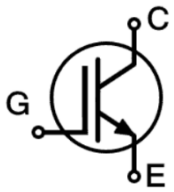

Fig. 5.2 IGBT circuit symbol

6. IGBT Switching Characteristics

One of the main important performance features of any semiconductor switching device is its switching characteristics. Understanding the device switching characteristics greatly improves its utilization in the various applications. The main performance switching characteristics of power semiconductor switching devices are the turn-on and turn-off switching transients in addition to the safe operating area (SOA) of the device.

Since most loads are inductive in nature, which subjects devices to higher stresses, the turn-on and turn-off transients of the IGBT are obtained with an inductive load test circuit as shown in Fig. 2.3. The load inductance is assumed to be high enough so as to hold the load current constant during switching transitions. The freewheeling clamp diode is required to maintain current flow in the inductor when the device under test (DUT) is turned off (Salman Jasim Hammoodi, 2020).

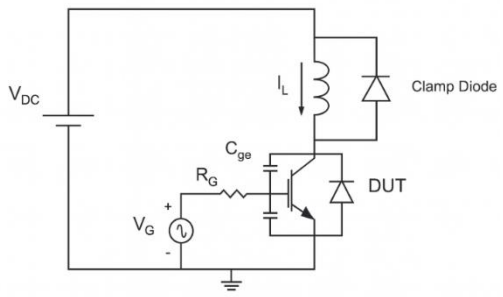

Fig. 6.1 Inductive load test circuit

Table -1: The physical parameters for DC motor

Moment of inertia of the rotor (J)	0.01 kg.m²
Motor viscous friction constant (b)	0.1 N.m.s
Electromotive force constant (K_e)	0.01 V/rad/sec
Motor torque constant (K_t)	0.01 N.m/Amp
Electric resistance (R)	1 Ohm
Electric inductance (L)	0.5 H

Transfer Function Equation of Feedback Control System The torque generated by a DC motor is proportional to the armature current and the strength of the magnetic field. In this example we will assume that the magnetic field is constant. Therefore, the motor torque is proportional to only the armature current by a constant factor K_t as shown in the equation below. This is referred to as an armature-controlled motor.

$$T = K_t\, i \qquad \text{(iii)}$$

Where T= torque, K_t= constant factor, i = armature current

The back emf e , is proportional to the angular velocity of the shaft by a constant factor K_e .

$$e = K_e\theta \qquad \text{(iv)}$$

Where: e= back e.m.f, K_e = constant factor, θ = angular velocity

In SI units, the motor torque and back e.m.f constants are equal, that is $K_t = K_e$; therefore, we will use to represent both the motor torque constant and the back e.m.f constant. From the figure above, we can derive the following governing equations based on Newton's 2nd law and Kirchhoff's voltage law.

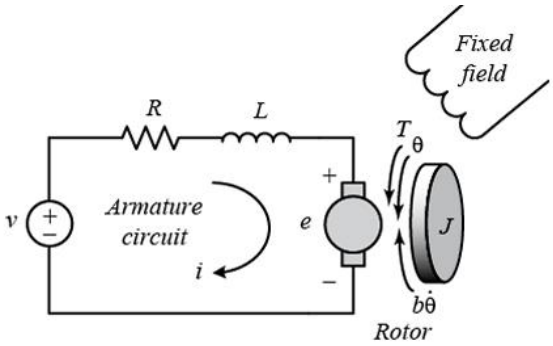

Fig 6.2 The electric equivalent circuit of the rotor

The electric equivalent circuit of the armature and the free body diagram of the rotor are shown in the following figure The input of the system is the voltage source (V) applied to the motor's armature, while the output is the rotational speed of the shaft $\frac{d\theta}{dt}$. The rotor and shaft are assumed to be rigid. A viscous friction model, that is, the friction torque is proportional to shaft angular velocity.

7. Block Diagram

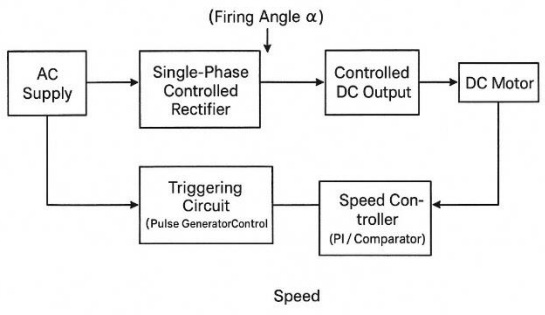

Fig. 7

The AC supply is fed to an SCR-based controlled rectifier. The triggering circuit adjusts the firing angle (α) and controls the output DC voltage. This voltage is applied to the DC motor armature, which changes its speed. A speed sensor measures the motor speed and sends feedback. The controller compares actual speed with reference and updates the firing angle (Shashi Bhushan Kumar, 2014).

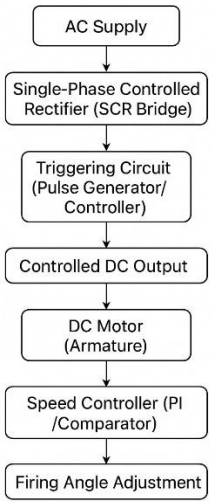

Fig. 7.1

8. Circuit Diagram and Discussion

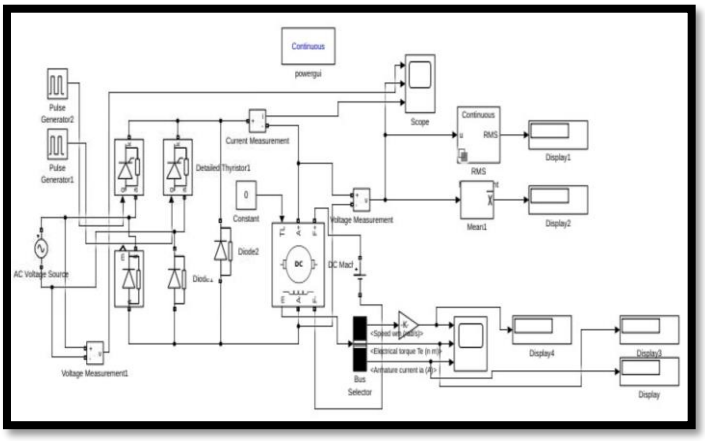

Fig. 8.1

The Simulink model shows controlling the speed of a DC motor using an SCR-based controlled rectifier. On the left side of the model, two pulse generators (Pulse Generator 1 and Pulse Generator 2) are used to produce gate-triggering signals for the thyristor blocks. These gate pulses determine the firing angle, which controls when the SCRs start conduction during each AC cycle.

Just below the pulse generators is the AC voltage source, which provides the input sinusoidal supply to the rectifier circuit. Multiple SCR and diode components are interconnected in a bridge configuration, forming a controlled rectifier that converts AC input into a variable DC output. In the central part of the diagram, the output of the rectifier is fed into a DC machine block representing the DC motor. This block models the motor's internal electrical and mechanical behavior such as armature current, torque, and rotational speed. The simulation also includes voltage measurement, current measurement, and RMS blocks that capture the electrical characteristics of the motor in real time.

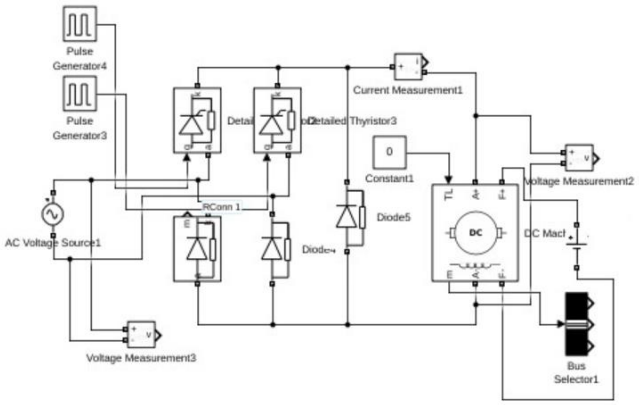

Fig. 8.2

A powergui block, set to Continuous mode, ensures that the power electronics elements (SCRs and diodes) and motor model are solved correctly using continuous-time equations. To the right of the motor block, a Bus Selector extracts three key output parameters from the DC motor: speed (in rad/s), electrical torque (in N·m), and armature current (in amperes). These outputs are fed into individual display blocks and scopes, allowing users to monitor the motor's dynamic response visually during simulation.

Additional RMS and Mean blocks calculate the effective voltage and average speed, which are also shown through display units for better interpretation of performance under different firing angles. Overall, the model clearly represents the entire control workflow from AC input to DC motor output. It visually demonstrates how varying the triggering pulses affects rectifier conduction, which in turn changes the armature voltage and motor behavior. The interconnected measurement blocks, scopes, and displays help in analyzing the speed, torque, and current variations, making this Simulink model an effective tool for understanding SCR-based DC motor speed control.

In addition to its functional layout, the Simulink model is designed to provide a clear visualization of how each subsystem interacts within the overall control strategy. The placement of elements from

firing circuits to motor feedback loops illustrates the sequential flow of electrical energy and signal information.

This structure allows users to trace the transformation of AC input into controlled DC power, observe how the firing angle directly influences motor parameters, and monitor system stability under different operating conditions.

Table 2

Sr. No	Alpha	First Gate Pulse	Second Gate Pulse	Speed	Torque	Armature
1	30	1.66×10^{-3}	210	995.6	265.3	215
2	60	3.33×10^{-3}	240	796.5	212.2	172
3	90	5×10^{-3}	270	597.4	159.2	129
4	120	6.66×10^{-3}	300	398.2	106.1	86
5	150	8.33×10^{-3}	330	199.1	53	43

The table 1 presents the variation in DC motor performance for different firing angles applied to an SCR-based controlled rectifier. As the firing angle (α) increases from 30° to 150°, a systematic reduction in motor input voltage is observed, which directly influences the motor's dynamic characteristics. The gate pulse delay increases proportionally with α, reflecting the delayed conduction interval of the SCRs. This reduction in effective DC voltage results in a progressive decrease in the motor's speed, as indicated by the drop from 995.6 rpm at α = 30° to just 199.1 rpm at α = 150°. The trend confirms the expected behavior of phase-controlled DC drives, where higher firing angles r strict the conduction period, lowering the average output voltage delivered to the armature.

A similar declining pattern is evident in the motor torque and armature current as the firing angle increases. The torque decreases from 265.3 N·m at α = 30° to 53 N·m at α = 150°, demonstrating the strong dependence of motor torque on the available armature voltage and current. Correspondingly, the armature current also reduces significantly, from 215 A to 43 A over the same α range.

These results clearly indicate that both torque and current follow the decreasing voltage profile generated by delayed SCR triggering. The overall analysis reinforces that firing angle control provides an effective method of regulating motor performance, enabling smooth variation of speed and torque for applications requiring precise and flexible control.

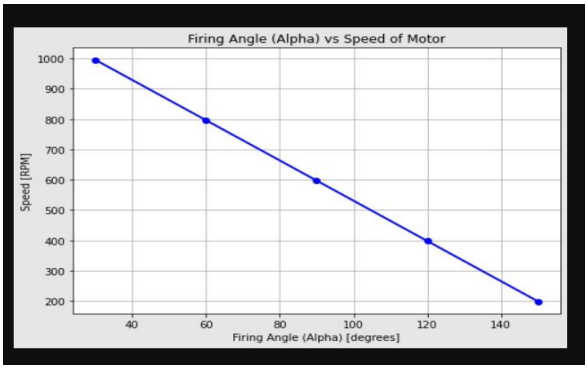

Fig. 8.3

The image shows a two-dimensional line graph illustrating the relationship between the firing angle (Alpha) of an SCR-controlled rectifier and the resulting speed of a DC motor.

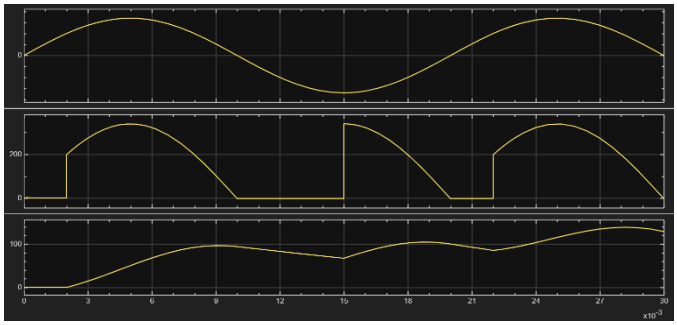

Fig. 8.4

The graph shows a clear, almost linear negative correlation between firing angle and motor speed. At the lowest firing angle of 30°, the motor achieves its maximum speed of approximately 1000 RPM. As the firing angle increases to 60° and 90°, the speed decreases progressively to around 800 RPM and 600 RPM, respectively.

Further increments to 120° and 150° reduce the speed sharply to about 400 RPM and 200 RPM. This downward trend visually highlights the direct impact of firing angle delay on reducing the average DC voltage supplied to the motor.

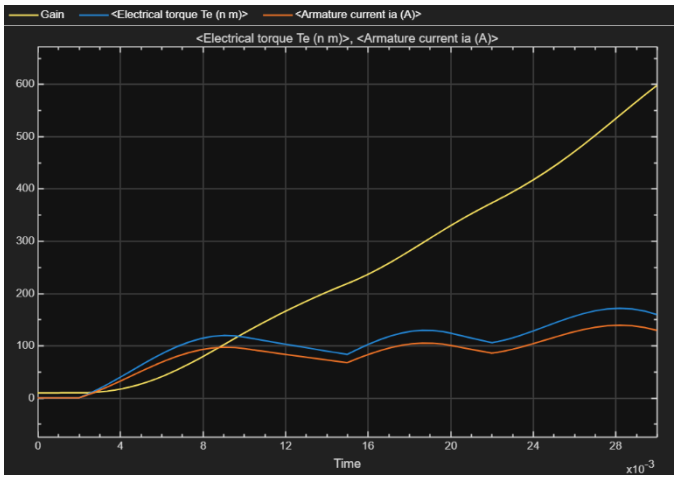

Fig. 8.5

The graph displays how electrical torque (Te), armature current (Ia), and gain change over time. Similar patterns can be seen in the armature current and electrical torque curves. Both start out rapidly, peak at 8–10 ms, and then exhibit slight oscillations over time. Their values continue to be between 80 and 170 units.

Compared to the other two, the gain curve exhibits distinct behavior. It begins at zero and increases steadily over the course of the entire duration. The gain reaches a value near 600 by the end of the plot, exhibiting an uninterrupted upward trend. Overall, the figure shows how the gain increases smoothly over time while torque and current change dynamically.

9. Future Scope

The scope will also cover the development of graphical outputs required to ascertain operating trends and performance limitations, such as speed versus firing angle, torque versus firing angle, and armature current versus firing angle. This work is meant to highlight the effectiveness of SCR-based control in industry through comparisons of simulated results versus expected theoretical characteristics.

The paper also identifies some of the limitations with phase-controlled approaches and suggests areas of future improvement involving the use of PWM drives, closed-loop control, or better controller integration using PID, fuzzy logic, or machine learning-based tuning.

10. Conclusion

It can be concluded that, the speed of DC motors can be controlled by using a thyristor, which is recognized as the full controlled rectifier and the design of our project meets the requirements in term of size and cost effectiveness. Moreover, some additional enhancements were made to the
To examine the speed control of DC motor, the software package MATLAB/ SIMULINK was used to design the block diagrams and run the simulations. The first point discussed in this work was the description of the operation of a DC motor, where the different aspects related to its operation were analyzed, and the parameters that influence the speed control of them.

We have successfully implemented and simulate the Speed of a DC motor is controlled by changing the firing angle (α) of a thyristor based controlled rectifier. The rectifier converts AC to controlled DC, and the amount of DC voltage supplied to the motor depends on the firing angle (Zainab B. Abdullah 1, 2023).

$$V_{avg} = \frac{V_m}{\pi}(1 + cos \propto)$$

$$Where, \quad V_m = AC\ Voltage$$
$$\propto = Firing\ Angle$$

Small firing angle (α ↓) → High DC voltage → Motor speed increases.

Large firing angle (α ↑) → Low DC voltage → Motor speed decreases.

References

1. Abdessamad Intidam, H. E. (2023). Development and Experimental Implementation of Optimized PI-ANFIS Controller for Speed Control of a Brushless DC Motor in Fuel Cell Electric Vehicles. Energies
2. Al-Falahi1, M. D. (2008). SPEED CONTROL OF A EPARATELY EXCITED DC MO TOR. American Journal of Applied Sciences, 227-233.
3. Arpita Banik, J. U. (2023). Speed Control of Single-Phase Induction Motor using TRIAC and Bluetooth Device. International Conference on Industrial Electronics: Developments & Applications (pp. 516-521). Institute of Electrical and Electronics Engineers Inc.
4. George, M. (2008). Speed Control of Separately Excited DC Motor. American Journal of Applied Sciences (pp. 227-233). Melaka, Malaysia: Science Publications.
5. Hashmia S. Dakheel1, Z. B. (2022). Simulation model of ANN and PID controller for direct current servo motor by using Matlab/Simulink. Telkomnika (Telecommunication Computing Electronics and Control), 922-932.
6. Ling Xu, J.-G. S.-Q. (2016). Brushless DC Motor Speed Control System Simulink Simulation . IEEE International Conference on Power and Renewable Energy (p. 5). Beijing, China : IEEE Press.
7. M. SRI-JAYANTHA, G. F. (1984). SCR-Controlled DC-Motor Model for an Electric Vehicle Propulsion System Simulation. IEEE TRANSACTIONS ON INDUSTRIAL ELECTRONICS.
8. Mrs Khin Ei Ei Khine, M. W. (2019). Simulation DC Motor Speed Control System by using PID Controller . International Journal of Trend in Scientific Research and Development.
9. Salman Jasim Hammoodi, K. S. (2020). Design and implementation speed control system of DC Motor based on PID control and Matlab Simulink. International Journal of Power Electronics and Drive System , 127-134.
10. Shashi Bhushan Kumar, M. H. (2014). Design and Simulation of Speed Control of DC Motor by Fuzzy Logic Technique with Matlab/Simulink. International Journal of Scientific and Research Publications, (p. 4). Patna, India.
11. W, C. T. (1991). A Fast-Response Current Controller for Microprocessor-Based SCR-dc Motor Drives. IEEE TRANSACTIONS ON INDUSTRY APPLICATIONS (p. 7). IEEE.
12. Zainab B. Abdullah 1, S. W. (2023). Simulation Model of PID Controller for DC Servo Motor at Variable and Constant Speed by Using MATLAB. Journal of Robotics and Control (JRC), 54-59.